for methane elimination, whereas rearrangement via **6**, **2**, and **4** would produce CH_2DCHO, which would *not*. It would be of interest to see whether experimental isotope effects support the lower energy two-step pathway or the higher energy one-step rearrangement of **3** to **1**.

Our calculations indicate that elimination of molecular hydrogen from acetaldehyde[30] via transition structure **9** has a marginally lower energy requirement (339 kJ mol^{-1}) than the methane elimination via **7** (347 kJ mol^{-1}).

Concluding Remarks

(i) We find that vinyl alcohol (**2**) lies 47 kJ mol^{-1} higher and hydroxyethylidene (**3**) 213 kJ mol^{-1} higher in energy than acetaldehyde.

(ii) Hydroxyethylidene (**3**), although a high-energy species, is predicted to be separated by significant barriers (118 and 98 kJ mol^{-1}, respectively) from its lower energy isomers **1** and **2**; it should thus be observable, consistent with experiment.

(iii) The energy ordering of the transition structures (**4**, **5**, and **6**, respectively) for the rearrangements **1** → **2**, **1** → **3**, and **2** → **3** is **4** < **6** < **5**. This is in apparent conflict with conclusions based on experimental observations.

(iv) The rate-determining step for the production of CO from any of the three isomers **1**-**3** is predicted to correspond to the elimination of methane from acetaldehyde (**1**) (preceded in the case of both **2** and **3** by lower energy rearrangements to **1**), and this is consistent with isotope effects observed in NRMS studies.

Acknowledgment. We thank Professor Fred McLafferty for helpful discussions, Professor J. D. Goddard for providing us with results prior to publication, and gratefully acknowledge a generous allocation of time on the Fujitsu FACOM VP-100 of the Australian National University Supercomputer Facility.

Supplementary Material Available: Calculated (HF/6-31G(d)) vibrational frequencies for structures **1**-**9** (Table VII) (1 page). Ordering information is given on any current masthead page.

Extended Molecular Mechanics Calculations of Thermodynamic Quantities, Structures, Vibrational Frequencies, and Infrared Absorption Intensities of Formic Acid Monomer and Dimer

Isao Yokoyama, Yoshihisa Miwa, and Katsunosuke Machida*

Contribution from the Faculty of Pharmaceutical Sciences, Kyoto University, Sakyo-ku, Yoshida, Kyoto 606, Japan. *Received January 22, 1991*

Abstract: The molecular mechanics simulation of infrared absorption spectra utilizing the effective atomic charges and charge fluxes as both the potential and the intensity parameters has been applied to formic acid monomer and dimer. The thermodynamic properties, optimized geometries, vibrational frequencies, and infrared absorption intensities are consistently derived from the potential models in which the difference between the monomer and the dimer is empirically taken into account. The large splitting between the A_g and the B_u cabonyl stretching frequencies of the dimer and the extension of the carbonyl bond on the dimerization are simultaneously reproduced by introducing two charge fluxes $\partial q_{O=C}/\partial r_{C=O}$ and $\partial q_{O-H}/\partial r_{C=O}$. The charge flux $\partial q_{OH}/\partial r_{OH}$ is responsible for the large frequency shift and intensification of the OH stretching band on the dimerization.

In our previous two reports,[1] an extended scheme of the molecular mechanics calculation was presented with illustrative simulations of vibrational spectra of *n*-alkanes and *n*-alkyl ethers. The empirical force field used in these works includes the Coulomb potential parameters in the form of effective charges of the atoms and their fluxes through the bonds on the change of bond lengths and valence angles (ECCF model[2]). The charge fluxes represent the deformability of the atomic charges during the nuclear motions.[2,3] These atomic charges and charge fluxes were used also as parameters for predicting the infrared absorption intensities. The enthalpies, entropies, and structures of *n*-alkanes and aliphatic ethers were successfully derived from this potential model.[1]

The present work has been undertaken to apply this method to formic acid monomer and dimer, which have been taken as suitable starting materials for dealing with the carboxyl group and hydrogen-bonded systems. Carboxylic acids are typical polar molecules, whose atomic charges and charge fluxes should play much more important roles in determining molecular structures and infrared absorption intensities than in the cases of *n*-alkanes and *n*-alkyl ethers. Formic acid is thus expected to afford severe criteria for testing whether any set of Coulomb potential parameters can elucidate the experimental data of these physical properties with reasonable accuracy. It is well known that carboxylic acid molecules are hydrogen-bonded pairwise to form cyclic centrosymmetric dimers. An estimation of the potential parameters and vibrational intensity parameters for such a system should be useful for further extension of our approach in molecular mechanics to compounds of biological interest.

Calculation

The potential model used in our approach[1] consists of six sums of terms each containing one or two variables. Each term in the

$$V = \sum_i D_i \exp\{-a_i(r_i - r_i^0)\}[\exp\{-a_i(r_i - r_i^0)\} - 2] + \sum_i \tfrac{1}{2}F_i(R_i - R_i^0)^2 + \sum_{i,j} F_{ij}(R_i - R_i^0)(R_j - R_j^0) + \sum_i \sum_n \tfrac{1}{2}V_{ni}\{1 - (-1)^n \cos n\tau_{ni}\} + \sum_{i,j} \tfrac{1}{2}V_{NB}(r_{ij}) + \sum_{i,j} \tfrac{1}{2}q_i q_j(1/\epsilon_{ij}r_{ij}) \quad (1)$$

first sum in eq 1 represents the Morse potential for the change of the bond length r_i. The parameters D_i were first taken as the standard bond energies calculated from the thermodynamic data in the literature,[4,5] and so adjusted as to fit the heat of formation

(1) (a) Machida, K.; Noma, H.; Miwa, Y. *Indian J. Pure Appl. Phys.* **1988**, *26*, 197. (b) Miwa, Y.; Machida, K. *J. Am. Chem. Soc.* **1988**, *110*, 5183. (c) Miwa, Y.; Machida, K. *Ibid.* **1989**, *111*, 7733.
(2) Decius, J. C. *J. Mol. Spectrosc.* **1975**, *57*, 348.
(3) Gussoni, M.; Castiglioni, C.; Zerbi, G. *J. Phys. Chem.* **1984**, *88*, 600.
(4) CODATA recommended key values for thermodynamics, 1977: *J. Chem. Thermodyn.* **1978**, *10*, 903.

0002-7863/91/1513-6458$02.50/0

of the trans conformer of the monomer to the experimental value.[6] The initial values were 0.762 for the OH in water,[4] 0.533 for the C–O in methanol,[5] 1.327 for the C=O in carbon dioxide[4] in the unit of aJ per molecule. The intrinsic bond lengths r_i^0 were firstly set equal to the sum of the covalent radii[7] and were slightly modified to explain the experimental bond lengths of the monomer.[8,9] The Morse functions estimated from the monomeric data were found to be transferable to the dimer when fitting of only the thermodynamic data and the structures was aimed at, but a slight modification of the parameters a_i was necessary for fitting the vibrational frequencies of the dimer closely.

In our earlier crystal packing analysis of simple amino acids[10] and aspirin,[11] the dependence of the energy on the hydrogen bond length was represented by the Lippincott function.[12] In this work, however, we adopted the Morse function for the stretching potential of the hydrogen bond in the carboxylic acid cyclic dimer, since the negative curvature of the Lippincott function in the short distance region was found to be unfavorable for the geometry optimization by the Newton–Raphson method.

Initially, the Morse parameters for the hydrogen bond were taken to give the same values of the bond distance, depth, and curvature at the minimum as previously used in the Lippincott function for aspirin.[11] These parameters were then adjusted by referring to the experimental values of the hydrogen-bonded distance r(O···O) (2.696 Å[8,9]) by electron diffraction, the dimerization enthalpy ΔH_D (−48.9 kJ mol^{-1} [13]) and entropy ΔS_D (−151.5 J mol^{-1} deg^{-1} [14]) by infrared spectroscopy, and the hydrogen-bond stretching frequencies ν(O···O) (248 cm^{-1} [15]).

The second and the third sums stand for a general valence-type quadratic potential for the difference between each structure parameter R_i and its intrinsic value R_i^0. The intrinsic valence angles were assumed first to be tetrahedral for the C–O–H and to be 120° for the other angles, and were adjusted iteratively to fit the calculated angles at the potential minima of the trans monomer and the dimer to the observed values.[8,9] To reproduce the vibrational frequencies, the general valence-type force constants for the formic acid dimer by Ovaska[16] were used as the initial values for the dimer. Those for the monomer were obtained by converting the Urey–Bradley force constants by Nakamoto and Kishida[17] into the internal coordinate space. They were refined by referring to the observed infrared and Raman frequencies and the infrared absorption intensities of four isotopic formic acids under the influence of contribution from the other sums in our potential model.

The fourth sum stands for the internal rotation potential around a single bond, written as a truncated Fourier series. The 2-fold torsional parameters for the O=C—O—H and H—C—O—H torsion angles of the monomer were so determined as to explain the experimental values of the energy difference[18] between the

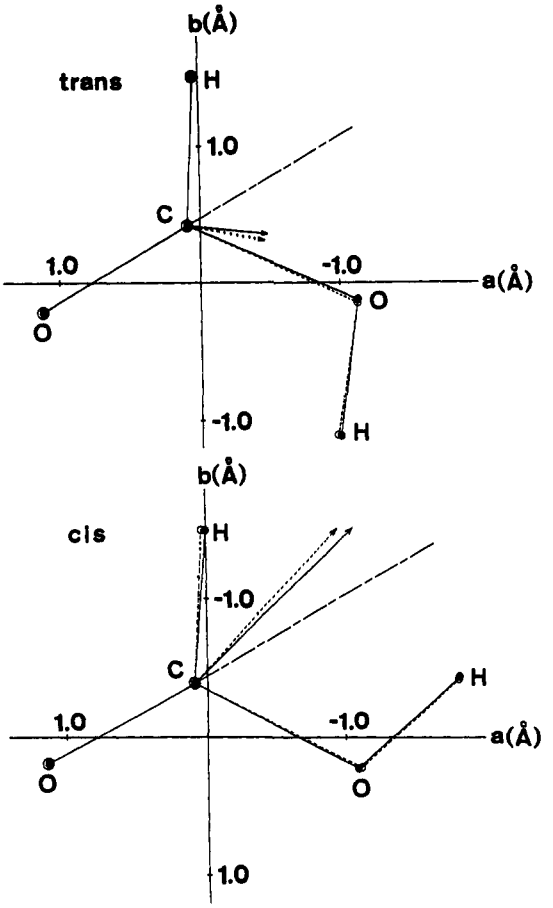

Figure 1. Calculated (full line) and observed (dotted line) dipole moment vectors μ of trans and cis conformers of formic acid monomer. The filled and the hollow circles indicate the calculated and the observed atomic coordinates, respectively.

trans and the cis conformers with respect to the C–O bond (see Figure 1), the rotational barrier about the C–O bond,[19,20] and the COH out-of-plane bending frequencies for the trans and the cis conformers.[18,21] The calculated barrier for the final parameters, 57.7 kJ mol^{-1}, is comparable with the observed values of 57.7 kJ mol^{-1} by microwave[19] and 56.1 kJ mol^{-1} by infrared spectroscopy.[20] Since there was no evident reason for distingushing between the parameters for the above two torsional angles, these were assumed as equal to each other. On the other hand, an additional torsional parameter around the C=O bond should be introduced for the dimer because the angle formed by the hydrogen bond C=O···H is bent. The two torsional parameters around the C—O and the C=O bonds were so adjusted as to fit the calculated frequencies of the OH out-of-plane deformation, the CO_2 wagging, and the CO_2 twisting modes of the dimer to the observed ones. The newly estimated potential parameters in the first through the fourth sums of eq 1 are summarized in Table I.

The fifth sum represents the modified Buckingham-type exchange repulsion–dispersion potential[1]. The same parameters as adopted previously for *n*-alkanes[1b] and *n*-alkyl ethers[1c] were used, since we found no positive reason for altering them for the hydrogen, carbon, and oxygen atoms of formic acid. The potential parameters for the geminal atom pairs were distinguished from those for the more distantly separated pairs, but the atom pairs separated by a covalent bond and a hydrogen bond were not regarded as geminal.

The last sum represents the Coulomb potential modified with an effective dielectric constant, ϵ_{ij}, which is taken to be 1.63 for

(5) Wagman, D. D.; Evans, W. H.; Parker, V. B.; Halow, I.; Bailey, S. M.; Schumm, R. H. *NBS Technical Note 270-3: Selected Values of Chemical Thermodynamic Properties, Tables for the First Thirty-Four Elements in the Standard Order of Arrangement*, U.S. Government Printing Office, Washington, DC, 1968.
(6) Pedley, J. B.; Naylor, R. D.; Kirby, S. P. *Thermochemical Data of Organic Compounds*, 2nd ed.; Chapman and Hall: London, 1986.
(7) Pauling, L. *The Nature of the Chemical Bond*; Cornell University: Ithaca, NY, 1960.
(8) Almenningen, A.; Bastiansen, O.; Motzfeldt, T. *Acta Chem. Scand.* **1969**, *23*, 2848.
(9) Harmony, M. D.; Laurie, V. W.; Kuczkowski, R. L.; Schwendeman, R. H.; Ramsay, D. A.; Lovas, F. J.; Lafferty, W. J.; Maki, A. G. *J. Phys. Chem. Ref. Data* **1979**, *8*, 619.
(10) Machida, K.; Kagayama, A.; Saito, Y. *J. Raman Spectrosc.* **1979**, *8*, 133.
(11) Kim, Y.; Machida, K.; Taga, T.; Osaki, K. *Chem. Pharm. Bull.* **1985**, *33*, 2641.
(12) Lippincott, E. R. *J. Chem. Phys.* **1953**, *21*, 2070.
(13) Henderson, G. *J. Chem. Educ.* **1987**, *64*, 88.
(14) Clague, A. D. H.; Bernstein, H. J. *Spectrochim. Acta* **1969**, *25A*, 593.
(15) Carlson, G. L.; Witkowski, R. E.; Fateley, W. G. *Spectrochim. Acta* **1966**, *22*, 1117.
(16) Ovaska, M. *J. Phys. Chem.* **1984**, *88*, 5981.
(17) Nakamoto, K.; Kishida, S. *J. Chem. Phys.* **1964**, *41*, 1554.
(18) (a) Hocking, W. H. *Z. Naturforsch.* **1976**, *31a*, 1113. (b) Bjarnov, E.; Hocking, W. H. *Z. Naturforsch.* **1978**, *33a*, 610.
(19) Winnewisser, B. P.; Hocking, W. H. *J. Phys. Chem.* **1980**, *84*, 1771.
(20) Bernitt, D. L.; Hartman, K. O.; Hisatsune, I. C. *J. Chem. Phys.* **1965**, *42*, 3553.
(21) Bertie, J. E.; Michaelian, K. H. *J. Chem. Phys.* **1982**, *76*, 886.

Table I. Potential Parameters

Bond Stretching

r_i	a_i, Å^{-1} monomer	a_i, Å^{-1} dimer	D_i, aJ	r_i^0, Å
H—C	1.9100	1.8680	0.6980	1.085
C—O	2.2423	2.3943	0.6010	1.330
C=O	2.2080	2.2453	1.3500	1.190
O—H	2.1401	2.1556	0.7755	1.000
O···H		1.5500	0.0480	1.670

Intrinsic Angles and General Quadratic Force Constants (Diagonal)

θ_i	θ_i^0, deg monomer	θ_i^0, deg dimer	F_i, aJ rad^{-2} monomer	F_i, aJ rad^{-2} dimer
C—O—H	102.5	107.0	0.5515	0.8898
O—C=O	124.0	126.0	1.3798	1.2800
H—C—O	110.5	117.0	0.5405	0.6040
H—C=O	125.5	117.0	0.6500	0.6500
O—H···O				
(in-plane)		0.0		0.0050
(out-of-plane)		0.0		0.1200
C=O···H		120.0		0.0400
CO_2 out-of-plane	0.0	0.0	0.4600	0.4850

General Quadratic Force Constants (Off-Diagonal)

symbol		F_{ij} monomer	F_{ij} dimer
stretching–stretching[a]	H—C, C—O	0.4590	0.2130
	H—C, C=O	0.3369	0.2230
	C—O, O—H	0.4067	0.2660
	O—C, C=O	0.2916	0.5000
stretching–bending[a]	H—C—O, H—C	0.3659	0.0000
	H—C—O, C—O	0.5674	0.2330
	H—C=O, H—C	0.4250	0.0000
	H—C=O, C=O	0.5970	0.4560
	H—O—C, O—H	0.0369	0.1810
	H—O—C, C—O	−0.0817	0.2140
	O—C=O, C—O	0.3849	0.2000
	O—C=O, C=O	0.0111	0.2880
bending–bending[a]	H—O—C, O—C=O	−0.4358	0.0000
	H—C—O, C—O—H	−0.1246	0.0000

Torsion Potential Parameters

τ_{2i}	V_{2i}, 10^{-2} aJ monomer	V_{2i}, 10^{-2} aJ dimer
O=C—O—H, H—C—O—H	4.440	2.100
O—C=O···H, H—C=O···H		0.600

[a] The stretching–stretching constants in N cm^{-1}, the stretching–bending constants in 10^{-8} N rad^{-1}, the bending–bending constants in aJ rad^{-2}.

the vicinal atom pairs, and 1.0 for the atom pairs separated by more than two atoms.[1] The geminal atom pairs are not included in the sum. The modification of ϵ_{ij} is necessary for simultaneous fitting of the heat of dimerization and the dipole moments of the monomeric trans and cis conformers. The hydrogen bond is not taken into account on picking up the atom pairs for which the Coulomb interaction is to be processed in the particular ways described above according to the number of the bonds formed between them. The effective atomic charge q_i is expressed by:

$$q_i = q_i^0 + \sum_j \frac{\partial q_i}{\partial R_j}(R_j - R_j^0) \tag{2}$$

In eq 2, q_i^0 is the ith intrinsic atomic charge defined as the charge born by the atom i when all the bonds and the angles around it are fixed at their intrinsic values, and $\partial q_i/\partial R_j$ is the atomic charge flux with respect to the jth structure parameter evaluated at $R_j = R_j^0$. The instantaneous charge q_i corresponds to the "effective charge" introduced by King, Mast, and Blanchette.[22] The intrinsic charges were calculated from the atomic electronegativities, χ_k

(22) King, W. T.; Mast, G. B.; Blanchette, P. P. *J. Chem. Phys.* **1972**, *56*, 4440.

Table II. Bond Charge Parameters and Charge Fluxes in Formic Acid

symbol[a]	monomer	dimer
Bond Charge Parameters β, [b]e		
H—C	0.2131	0.2131
C—O	0.0193	0.0193
C=O	0.3187	0.3187
O—H	0.2390	0.1300
Bond Stretching Fluxes, [b]e Å^{-1}		
$\partial q_{CH}/\partial r_{HC}$	−0.191	−0.113
$\partial q_{OH}/\partial r_{HO}$	−0.110	0.721
$\partial q_{O-C}/\partial r_{C-O}$	0.660	0.757
$\partial q_{O=C}/\partial r_{C=O}$	0.697	0.850
$\partial q_{O\cdots H}/\partial r'_{C=O}$		0.240
Angle Bending Fluxes, [b]e rad^{-1}		
CO_2 Group		
$\partial q_{C-O}/\partial\theta_{O-C=O}$	0.0	0.130
$\partial q_{C-O}/\partial\theta'_{H-C=O}$	0.0	−0.065
$\partial q_{C-O}/\partial\theta_{H-C-O}$	0.0	−0.065
COH Group		
$\partial q_{OH}/\partial\theta_{COH}$	0.050	0.050
$\partial q_{O-C}/\partial\theta_{COH}$	0.050	0.050

[a] The meanings of the symbols are the same as those in previous papers (ref 1). [b] e = electronic unit.

and χ_i, and the bond charge parameters, β_{ki} by using eq 3 with the sum over the atoms bonded to atom i.[1]

$$q_i^0 = \sum_k \beta_{ki}(\chi_k - \chi_i) \tag{3}$$

The Pauling electronegativities[7] were used for the carbon and the hydrogen atoms. The same electronegativity for the oxygen atoms as used in our previous work[1c] on *n*-alkyl ethers, 3.60, was adopted in this work. Each term in the right side of eq 3 conceptually corresponds to the "effective bond charge" introduced by van Straten and Smit,[23] and the procedure of eq 3 is a simple modification of Del Re's method.[24] The values of β_{ki} were so determined as to make the effective atomic charges consistent with the absolute value and the direction of the experimental dipole moment[25] and the observed infrared absorption intensity of the COH out-of-plane bending mode of the monomeric trans conformer.[26] Note that the dipole moment is calculated by using the effective atomic charges and the geometry after the energy minimization. For the trans conformer, the calculated dipole moment was 1.446 D (obsd 1.415 ± 0.01 D[25]) and the angle between the dipole moment vector and the C=O bond was calculated to be 37.0° (obsd 42.4 ± 2° [25]). The calculated dipole moment for the cis conformer (4.01 D) is close to the observed values (3.79 D[18a]), and the direction agrees well with the observed one. The calculated and the observed dipole moment vectors of both the conformers are compared with each other in Figure 1. The bond charge parameters determined in this way are shown in Table II, together with the bond charge fluxes to which the atomic charge fluxes are related by:

$$\frac{\partial q_i}{\partial R_{ij}} = \frac{\partial q_{ji}}{\partial R_{ij}} - \sum_m \frac{\partial q_{im}}{\partial R_{ij}} \tag{4}$$

Here $\partial q_{ji}/\partial R_{ij}$ denotes the bond charge flux from atom j to atom i associated with the unit increase of the stretching coordinate R_{ij}. The sum in eq 4 is taken over the atoms directly bonded to atom i except atom j, on the condition that the change of R_{ij} does not give rise to any charge flow along a bond not directly attached to either i or j. Under the restriction of eq 3, the total charge is conserved on the change of R_{ij} by:

$$\frac{\partial q_{ij}}{\partial R_{ij}} = -\frac{\partial q_{ji}}{\partial R_{ij}} \tag{5}$$

(23) van Straten, A. J.; Smit, W. M. A. *J. Mol. Spectrosc.* **1976**, *62*, 297.
(24) Del Re, G. *J. Chem. Soc.* **1958**, 4031.
(25) Kim, H.; Keller, R.; Gwinn, W. D. *J. Chem. Phys.* **1962**, *37*, 2748.
(26) Marêchal, Y. *J. Chem. Phys.* **1987**, *87*, 6344.

Table III. Experimental and Calculated Equilibrium Geometries, Heats of Formation, and Entropies for Formic Acid

	monomer					
	trans		cis		dimer	
geometry[a]	exptl[b]	calcd	exptl[c]	calcd	exptl[d]	calcd
r H—C	1.097	1.096	1.105	1.096	1.079	1.089
r C—O	1.343	1.334	1.352	1.338	1.320	1.322
r C=O	1.202	1.204	1.195	1.199	1.217	1.223
r O—H	0.972	1.000	0.956	0.999	1.033	1.043
r O···O[e]					2.696	2.707
r O···O[f]					2.262	2.277
∠C—O—H	106.3	106.8	109.7	109.2	108.5	109.1
∠O—C=O	124.6	125.3	122.1	121.6	126.2	126.9
∠H—C—O	109.1[g]	110.8	114.6	113.5		117.2
∠H—C=O	124.1	123.9	123.2	124.9	115.4	115.9
∠O—H···O					172.7[h]	170.6
∠C=O···O					127.1[i]	129.8
	Heat of Formation and Entropy (at 298.15 K)					
$\Delta H_f°$[j]	−378.7[k]	−378.8	−362.4[l]	−363.1	−403.2[m]	−403.4
S[j]	249[n]	248		249	173[m]	169

[a] Bond distances in Å, angles in deg. [b] Experimental structure is that chosen by Harmony et al., ref 9. [c] Bjarnov and Hocking, ref 18b. [d] From ref 8 and the compilation by Harmony et al., ref 9. [e] Hydrogen-bonded distance in the dimer. [f] The intramolecular distance between the oxygen of the hydroxyl group and that of the carbonyl group. [g] Almenningen et al., ref 8. [h] The calculated value (DZ + P SCF) by Chang et al., ref 28. [i] The calculated value (6-31G** level) by Damewood et al., ref 29. [j] Heats of formation in kJ mol^{-1} and entropies in J mol^{-1} deg^{-1}. [k] Pedley, et al., ref 6. [l] The sum of the heat of formation of the trans conformer and the trans–cis energy difference (16.3 kJ mol^{-1} in ref 18a). [m] Estimated from the enthalpy ΔH_D (ref 13) and the entropy ΔS_D (ref 14) of dimerization. [n] Stull et al., ref 30.

Note that the restriction mentioned above is to be satisfied with respect to the intermolecular charge flows as well as to the intramolecular ones. Moreover, the redundancy among the three bending coordinates, $\theta_1 \sim \theta_3$, around an sp^2 carbon atom leads to the relation:

$$\sum_{j=1}^{3} \frac{\partial q_l}{\partial \theta_j} = 0 \qquad (6)$$

Initially, the charge fluxes were estimated in such a way as to fit the calculated intensities to the observed data.[26,27] Since the introduction of the charge fluxes into the potential produced more or less shifts of the calculated frequencies, it was necessary to adjust the other potential parameters accordingly. About 20 cycles of alternate adjustment of the charge fluxes and the other potential parameters led finally to a tolerable fit of both the frequencies and the intensities.

Results and Discussion

The structure parameters of the trans and the cis conformers of the monomer and the dimer after the energy minimization are shown in Table III. The calculated values are in reasonable agreement with experiment.[8,9] In spite of the same intrinsic bond lengths for the monomer and the dimer, the calculated changes of the bond lengths on the dimerization follow the observed trend very well. On the other hand, since the effect of the geminal nonbonded interaction on the coplanar valence angles cancel each other, the observed difference in the valence angles between the monomer and the dimer cannot be reproduced without assuming the corresponding difference in the intrinsic angles. The geometrical changes on the trans–cis conversion were reproduced very well although we did not refer to the structure data of the cis conformer[18] in the course of refinement of the potential parameters. The calculated values of the heats of formation and entropies of the monomer and the dimer agreed well with the experimental values as shown in Table III.

The calculated values of the vibrational frequencies and the infrared absorption intensities of the monomer and the dimer of formic acid and its deuterated analogues are compared with the experimental values in Tables IV and V, respectively. The calculated intensities for each isotope of the monomer and the dimer follow the overall order of magnitudes of the experimental values. The calculated frequency shifts on the deuteration reproduced the trend of observed isotope effects, giving the mean absolute differences between ν_{cal} and ν_{obs} of 12.5 cm^{-1} and 13.7 cm^{-1} for the monomer and dimer, respectively. Furthermore, the calculated frequency of the COH out-of-plane bending mode for the monomeric cis conformer (560 cm^{-1}) is in good agreement with the experimental value (553 cm^{-1} [18a]) by microwave spectra.

In Table VI, the effective charges calculated at the potential minimum in this work are compared with those estimated by previous investigators.[41-44] As a whole, our effective charges are close to those reported by Lifson et al.[44] (their 12-6-1 set III). These authors' values were estimated empirically by referring to the crystal structure, sublimation energy, dipole moment and dimerization energy. The ab initio values[41-43] seem to be overestimated, but the variations of our charges on the dimerization show the same tendency as predicted by the ab initio calculations except for the atomic charges on the hydroxyl group. The infrared absorption intensities of the OH stretching mode and the OH out-of-plane deformation mode are important for determination of the effective charges of the oxygen and the hydrogen atoms in the hydroxyl group and the OH stretching charge flux empirically. If the bond charge parameter β_{OH} (0.239) of the monomer is transferred to the dimer, the calculated intensity of the infrared absorption band due to the OH out-of-plane bending mode of the dimer becomes about three times as strong as the observed

(27) (a) Bournay, J.; Maréchal, Y. *Spectrochim. Acta* **1975**, *31A*, 1351. (b) Berckmans, D.; Figeys, H. P.; Geerlings, P. *J. Phys. Chem.* **1988**, *92*, 61. (c) Berckmans, D.; Figeys, H. P.; Maréchal, Y.; Geerlings, P. *Ibid.* **1988**, *92*, 66.
(28) Chang, Y. T.; Yamaguchi, Y.; Miller, W. H.; Schaefer, H. F., III *J. Am. Chem. Soc.* **1987**, *109*, 7245.
(29) Damewood, J. R., Jr.; Kumpf, R. A.; Mühlbauer, W. C. F.; Urban, J. J.; Eksterowicz, J. E. *J. Phys. Chem.* **1990**, *94*, 6619.
(30) Stull, D. R.; Westrum, E. F., Jr.; Sinke, G. C. *The Chemical Thermodynamics of Organic Compounds*; Wiley: New York, 1969.
(31) Crawford, B., Jr. *J. Chem. Phys.* **1958**, *29*, 1042.
(32) Hisatsune, I. C.; Heicklen, J. *Can. J. Spectrosc.* **1973**, *18*, 135.
(33) Millikan, R. C.; Pitzer, K. S. *J. Chem. Phys.* **1957**, *27*, 1305.
(34) Bertie, J. E.; Michaelian, K. H.; Eysel, H. H.; Hager D. *J. Chem. Phys.* **1986**, *85*, 4779.
(35) Marmar, E. B.; Pouchan, C.; Chaillet, M. *J. Chim. Phys.* **1979**, *76*, 1125.
(36) Miyazawa, T.; Pitzer, K. S. *J. Chem. Phys.* **1959**, *30*, 1076.
(37) Millikan, R. C.; Pitzer, K. S. *J. Am. Chem. Soc.* **1958**, *80*, 3515.
(38) Clague, D.; Novak, A. *J. Mol. Struct.* **1970**, *5*, 149.
(39) Hayashi, S.; Umemura, J.; Kato, S.; Morokuma, K. *J. Phys. Chem.* **1984**, *88*, 1330.
(40) Excoffon, P.; Maréchal, Y. *Spectrochim. Acta* **1972**, *28A*, 269.
(41) Bosi, P.; Zerbi, G.; Clementi, E. *J. Chem. Phys.* **1977**, *66*, 3376.
(42) Cox, S. R.; Williams, D. E. *J. Comput. Chem.* **1981**, *2*, 304.
(43) Dybal, J.; Cheam, T. C.; Krimm, S. *J. Mol. Struct.* **1987**, *159*, 183.
(44) Lifson, S.; Hagler, A. T.; Dauber, P. *J. Am. Chem. Soc.* **1979**, *101*, 5111.

Table IV. Experimental and Calculated Vibrational Frequencies and Infrared Absorption Intensities for Trans Conformers of Monomeric Formic Acid and Its Deuterated Species

		freq[a]		IR int[b]		
		exptl	calcd	exptl	calcd	assignments[c]
				HCOOH		
A′	ν_1	3569[d]	3584	60.6[e]	67.6	O—H
	ν_2	2942[d]	2952	35.3[e]	36.0	C—H
	ν_3	1777[d]	1776	231[e]	315	C=O
	ν_4	1381[d]	1415		0.8	H—C—O
	ν_5	1223[f]	1239	14.6[e]	4.7	C—O—H
	ν_6	1104[d]	1114	199[e]	191	C—O
	ν_7	625[d]	635	[g]	21.3	O—C=O
A″	ν_8	1033[h,f]	1032		0.7	H—C—O opb
	ν_9	642[d]	646	163[e,g]	155	C—O—H opb
				HCOOD		
A′	ν_1	2938[i]/2942[i]	2952	47[j]	35.6	C—H
	ν_2	2631[i]	2609	45[j]	38.3	O—D
	ν_3	1773[i]	1766	244[j]	292	C=O
	ν_4	1368[i]	1378		0.7	H—C—O
	ν_5	1178[i]	1164		123	C—O
	ν_6	972[f]	985		48.3	C—O—D
	ν_7	560[i]	567		24.6	O—C=O
A″	ν_8	1011[i]	1029		0.0	H—C—O opb
	ν_9	508[f]	510		92.8	C—O—D opb
				DCOOH		
A′	ν_1	3566[i]	3584	87[j]	67.6	O—H
	ν_2	2218[i]	2191	77[j]	63.8	C—D
	ν_3	1760[i]/1724[i]	1734	302[j]	283	C=O
	ν_4	1297[i]	1310		0.9	C—O—H
	ν_5	1140[i]	1112		188	C—O
	ν_6	970[h]	974		0.5	D—C—O
	ν_7	620[i]	631		21.3	O—C=O
A″	ν_8		868		1.9	D—C—O opb
	ν_9	629[h]	637		151	C—O—H opb
				DCOOD		
A′	ν_1	2632[d]	2609	36.9[e]	38.0	O—D
	ν_2	2232[d]	2189	55.6[e]	60.3	C—D
	ν_3	1735[d]	1728	278[e]	265	C=O
	ν_4	1170[d]	1177	140[e]	77.8	C—O
	ν_5	1042[d]	1040	4.1[e]	77.0	C—O—D+D—C—O[k]
	ν_6	945[d]	932	56.8[e]	8.4	C—O—D+D—C—O[k]
	ν_7	556[d]	565	42.9[e]	24.5	O—C=O
A″	ν_8	873[h]	868		3.2	D—C—O opb
	ν_9	491[i]	493		86.3	C—O—D opb

[a] In cm^{-1}. [b] In km mol^{-1}. [c] Chang et al., ref 28; opb = out-of-plane bending. [d] Bertie and Michaelian, ref 21. [e] The observed IR intensity A_i (km mol^{-1}) of the ith normal mode is estimated by the following equation (ref 31): $A_i = 0.1\Gamma_i$ (m^2 mol^{-1})·$\bar{\nu}_i$ (cm^{-1}), where Γ_i and $\bar{\nu}_i$ are the intensity and the band center of the ith mode, respectively, observed by Marêchal (ref 26). [f] Hisatsune and Heicklen, ref 32. [g] The intensity sum of the O—C=O deformation and the C—O—H out-of-plane bending modes was estimated as the product of Γ in Table I and the average of the $\bar{\nu}$ of $\delta_{OC=O}$ and γ_{OH} modes in Table II of ref 26. [h] Millikan and Pitzer, ref 33. [i] Bertie et al., ref 34. [j] Berckmans et al., ref 27b. [k] Marmar et al., ref 35. [l] Miyazawa and Pitzer, ref 36.

intensity in the gas phase;[26] see Table VII. To reproduce the observed intensity in the dimer, we were compelled to reduce β_{OH} to 0.130, because no other parameters could effectively control the intensity of the OH out-of-plane deformation mode within the framework of the potential model used in this work. The reduction of β_{OH} led necessarily to unfavorable diminishing of the intrinsic effective charge on the hydroxyl oxygen atom, $q_O{}^0$, and that on the hydroxyl hydrogen atom, $q_H{}^0$, of the dimer. A preliminary survey of acetic acid and its higher homologue has led to the same conclusion. It is not conclusive at present if we can modify the potential model to allow for a reasonable increase of the intrinsic atomic charges on the hydroxyl group of the dimer without bringing forth any conflicts with the available experimental data.

According to the physical meaning of the sign of the charge flux,[45] the present result on the OH stretching vibration indicates

Table V. Experimental and Calculated Vibrational Frequencies and Infrared Absorption Intensities for Formic Acid Dimer and Its Deuterated Dimers

		freq[a]		IR int[b]			
		exptl	calcd	exptl		calcd	assignments[c]
				$(HCOOH)_2$			
A_u	ν_{13}	1050[d]	1057			0.0	δC—H opb
	ν_{14}	917[d]	917	s[d]	145[e]	136	δO—H opb
	ν_{15}	163[f]	183	m[f]		24.6	O—H···O opb
	ν_{16}	68[f]	74	w[f]		1.7	twist CO_2[g]
B_u	ν_{17}	3110[d]	3101	vs[d]	1980[e]	1942	O—H
	ν_{18}	2957[d]	2963	vs[d]	102[h]	122	C—H
	ν_{19}	1754[d]	1740	vs[d]	766[e]	716	C=O
	ν_{28}	1450[d]	1432	vw[d]		36.4	C—O—H
	ν_{21}	1365[d]	1384	m[d]	54.6[e]	23.9	H—C—O
	ν_{22}	1218[d]	1225	vs[d]	316[e]	299	C—O
	ν_{23}	697[d]	694	m[d]	47.6[e]	49.4	O—C=O
	ν_{24}	248[f]	245	s[f]		6.6	O···O[g]
				$(HCOOD)_2$			
A_u	ν_{13}	1037[d]	1056			0.4	δC—H opb
	ν_{14}	693[d]	669			83.3	δO—D opb
	ν_{15}	158[i]	179	s[i]		23.0	O—D···O opb
	ν_{16}	68[i]	73	m[i]		1.7	twist CO_2[g]
B_u	ν_{17}	2960[d]	2966	m[d]	94[h]	19.2	C—H
	ν_{18}	2314[d]/2068[j]	2254	s[d]	1050[h]	1118	O—D
	ν_{19}	1745[d]	1732	vs[d]	579[h]	687	C=O
	ν_{28}	1387[d]	1407	m[d]		57.8	H—C—O
	ν_{21}	1259[d]	1232	s[d]		272	C—O
	ν_{22}	1037[d]	1055	m[d]		10.5	C—O—D
	ν_{23}	651[d]	664	m[d]		51.2	O—C=O
	ν_{24}	240[i]	240	vs[i]		6.3	O···O
				$(DCOOH)_2$			
A_u	ν_{13}	930[d]	921	m,b[d]		127	δO—H opb
	ν_{14}	890[d]	890	m,b[d]		9.1	δC—D opb
	ν_{15}		154			17.8	O—H···O opb
	ν_{16}		74			1.7	twist CO_2[g]
B_u	ν_{17}	3098[d]	3099	s[d]	3280[h]	2029	O—H
	ν_{18}	2251[d]/2224[d]	2204	ms[d]/m[d]	154[h]	49.8	C—D
	ν_{19}	1726[d]	1724	s[d]	741[h]	791	C=O
	ν_{28}	1360[d]	1406	w[d]		4.9	C—O—H
	ν_{21}	1239[d]	1232	s[d]		200	C—O
	ν_{22}	996[d]	1007	m[d]		55.2	D—C—O
	ν_{23}	695[d]	687	m[d]		50.3	O—C=O
	ν_{24}		239			6.4	O···O
				$(DCOOD)_2$			
A_u	ν_{13}	890[d]	897	w, b[d]		9.5	δC—D opb
	ν_{14}	678[d]	663	s[d]	127[e,k]	73.4	δO—D opb
	ν_{15}	135[f]	152	w[f]		17.0	O—D···O opb
	ν_{16}	68[f]	73	w[f]		1.7	twist CO_2[g]
B_u	ν_{17}	2323[d]	2256	s, b[d]	795[e]	982	O—D
	ν_{18}	2226[d]	2200	s[d]	139[h]	170	C—D
	ν_{19}	1720[d]	1717	vs[d]	585[e]	761	C=O
	ν_{20}	1246[d]	1238	s[d]	195[e]	183	C—O
	ν_{21}	1055[d]	1055	w[d]	10.7[e]	2.9	C—O—D
	ν_{22}	987[d]/976[d]	1004	s[d]/s[d]	55.1[e]	56.3	D—C—O
	ν_{23}	642[d]	658	s[d]	k	51.9	O—C=O
	ν_{24}	227[f]	234	s[f]		6.1	O···O

[a] In cm^{-1}. [b] In km mol^{-1}. Abbreviations: vs, very strong; s, strong; ms, medium strong; m, medium; w, weak; vw, very weak; b, broad. [c] Chang et al., ref 28; opb = out-of-plane bending. [d] Millikan and Pitzer, ref 37. [e] The observed IR intensities were estimated on the basis of Marêchal's (ref 26) experimental data. See footnote *e* in Table IV. Here the dimer is regarded as a molecular unit. [f] Clague and Novak, ref 38. [g] Hayashi et al., ref 39. [h] Berckmans et al., ref 27c. [i] Carlson et al., ref 15. [j] Excoffon and Marêchal, ref 40. [k] The intensity sum of the O–D out-of-plane bending and the O—C=O deformation modes was estimated as the product of the Γ in Table I and the γ_{OD} band center in Table II of ref 26.

that the stretching of the OH bond of the monomer leads finally to the atomic dissociation, while the OH stretching in the dimer

(45) Mast, G. B.; Decius, J. C. *J. Mol. Spectrosc.* **1980**, *79*, 158.

Table VI. Atomic Net Charges of Formic Acid Monomer and Dimer

	net charges[a]						
	monomer				cyclic dimer		chain polymer
atom	this work	ref 41[b]	ab initio ref 42[c]	ref 43[c]	this work	ab initio ref 43[b]	empirical ref 44
H(HC)	+0.083	+0.169	+0.059	+0.144	+0.085	+0.184	+0.10
C	+0.305	+0.503	+0.674	+0.602	+0.308	+0.573	+0.28
O(C=O)	−0.360	−0.479	−0.628	−0.549	−0.386	−0.539	−0.38
O(C—O)	−0.390	−0.545	−0.568	−0.578	−0.242	−0.616	−0.38
H(OH)	+0.362	+0.352	+0.462	+0.381	+0.236	+0.390	+0.38

[a] In electronic units. [b] The 9s4p/4s basis set. [c] The 6-31G** basis set.

Table VII. Effects of Intrinsic Charges (q_O^0 and q_H^0) and OH Stretching Charge Flux ($\partial q_{OH}/\partial r_{OH}$) on Infrared Absorption Intensities of Dimeric OH Modes and Monomer–Dimer Variation

	calcd			
	case 1	case 2[a]	case 3	exptl
effective bond charge				
β_{OH}[b]	0.239	0.130	0.130	
intrinsic charges				
q_O^0[b]	−0.380	−0.216	−0.216	
q_H^0[b]	+0.359	+0.195	+0.195	
OH stretching charge flux				
$\partial q_{OH}/\partial r_{OH}$[c]	+0.721	+0.721	0.000	
ν_{OH}				
freq[d]	2976	3101	3571	3110[e]
IR int[f]	1226	1942	95	1980[g]
γ_{OH}				
freq[d]	993	917	926	917[e]
IR int[f]	385	136	105	145[g]
monomer–dimer variation				
frequency shift $\Delta\nu_{OH}$[d]	−608	−483	−13	−459[e,h]
geometrical change Δr_{OH}[i]	+0.056	+0.043	+0.006	+0.061[j]
intensity ratio (dimer/monomer)	9.1[k]	14.4[k]	0.7[k]	16.3[g,k]

[a] Note that case 2 corresponds to the results with the final force field. [b] In electronic unit. [c] In e Å^{-1}. [d] In cm^{-1}. ν_{OH} = OH stretching mode, γ_{OH} = OH out-of-plane bending mode. [e] Millikan and Pitzer, ref 37. [f] In km mol^{-1}. [g] Maréchal, ref 26. [h] Bertie and Michaelian, ref 21. [i] In Å. [j] Harmony et al., ref 9. [k] The intensity ratio was calculated by $(I_d/2)/I_m$, where I_d and I_m (km mol^{-1}) were taken from Tables IV and V, respectively.

leads to the ionic dissociation. The magnitude of our OH stretching charge flux in the monomer is of reasonable order in comparison with those in the related compounds.[3,46] The charge flux of the OH stretching in an isolated water molecule was estimated to be −0.216 e Å^{-1} by Yamaoka and Machida[46] and −0.22 e Å^{-1} by Gussoni et al.,[3] and the flux in isolated alcohol to be −0.11 e Å^{-1} by Gussoni et al.[3] on the basis of experimental data of the infrared absorption intensities. Our flux of −0.110 e Å^{-1} is equal to that in methyl alcohol and roughly half as large as that in water. Moreover, Dybal et al.[43] calculated the partial charge derivative $\partial q_H/\partial r_{OH}$ of formic acid monomer in the 6-31G** basis as −0.351 e Å^{-1}. Thus the negative sign of the flux in the monomer is regarded as reasonable. In the dimer, the large positive value of +0.721 e Å^{-1} was necessary for reproducing the large infrared absorption intensity of the OH stretching mode. Kim and Machida[47] empirically calculated the infrared absorption intensities of the benzoic acid dimer, by combining a simple charge flux model and the *L* matrix obtained by normal coordinate analysis. As a result, the OH stretching charge flux was estimated as +0.20 e Å^{-1}, with the sign comparable with ours. The magnitude of the flux by Kim and Machida[47] is smaller than ours because the estimated charges on the hydroxyl group are about one and a half times as large as ours. In respect of the C=O stretching charge flux, the sign estimated by Kim and Machida[47] is also the same as ours.

The effects of the intrinsic charges and the charge flux of the OH bond of formic acid dimer on the relevant spectroscopic quantities and the OH bond length are illustrated in Table VII. Compared with the case of its absence, it is evident that the large OH stretching charge flux is responsible for the low-frequency shift by about 480 cm^{-1} and the intensification by about 15 times that of the infrared absorption due to the OH stretching mode. The frequency shift reflects the fact that the second derivative of the Morse function decreases sensitively on a slight increase of the bond distance. On the other hand, the extention of the bond distance is favored energetically by the enhancement of the Coulomb attraction, since the positive charge flux increases the polarity of the bond as manifested in the marked intensification of the infrared absorption due to the OH stretching mode. According to a trial calculation, the OH stretching charge flux in the dimer stabilizes the Coulomb energy by 11.6 kJ mol^{-1} as compared with the case of its absence.

It is well known that carboxylic acids which form centrosymmetrical cyclic dimers exhibit a large splitting of 40 to 80 cm^{-1} between the A_g and B_u C=O stretching modes. Dybal et al.[43] ascribed this splitting to the change of the effective charge (charge flux) brought about by the large electrostatic interaction associated with the formation of a cyclic dimer. In this work, we tried to reproduce the splitting of the C=O stretching modes of formic acid dimer by introducing various charge fluxes on the stretching of the C=O bond, and finally found two effective fluxes $\partial q_{O=C}/\partial r_{C=O}$ and $\partial q_{O\cdots H}/\partial r_{C=O}$. Note that the latter flux represents a sort of charge transfer through the hydrogen bond. These charge fluxes are necessary also for fitting the absolute infrared absorption intensity of the B_u C=O stretching mode reported by Maréchal.[26]

Table VIII shows the effects of the two C=O stretching charge fluxes on the B_u–A_g splitting and the infrared absorption intensity of the B_u C=O stretching mode of the dimer. The frequency difference $\Delta\nu_{C=O}$ between the C=O stretching bands of the monomer and the dimer and the extension of the C=O bond on dimerization, $\Delta r_{C=O}$, are also given. Introduction of the two charge fluxes reproduced these quantities fairly well as compared with the case of the absence of both the fluxes. From the calculated values in the absence of each of the two fluxes, it is obvious that $\partial q_{O=C}/\partial r_{C=O}$ is fully responsible for the large infrared absorption intensity of the C=O stretching mode, and produces about half of its splitting in the dimer, whereas $\partial q_{O\cdots H}/\partial r_{C=O}$ alone shows little effect on both the intensity and the splitting. The latter flux contributes, however, very effectively to the enhancement of the B_u–A_g splitting of C=O stretching modes in cooperation with the former.

In terms of the general force field of the dimer, the B_u–A_g splitting of any modes may be attributed to the intermolecular force constants which couple the equivalent coordinates of the two monomer units. Thus it is worth clarifying what types of intermolecular valence force constants derive from the two charge fluxes introduced above. For this purpose, the force constants for the Cartesian coordinates were transformed to the internal coordinate space by means of the inverse *B* matrix obtained by dropping the O···H stretching and the O—H···O and C=O···H bending coordinates.[43] The reduction of the *B* matrix is necessary for avoiding the indeterminacy of certain force constants caused

(46) Yamaoka, Y.; Machida, K. *J. Mol. Spectrosc.* **1983**, *100*, 234.
(47) Kim, Y.; Machida, K. *Spectrochim. Acta* **1986**, *42A*, 881.

Table VIII. Effects of C=O Stretching Charge Fluxes on B_u–A_g Splitting, Infrared Absorption Intensity of B_u C=O Stretching Mode, and Monomer–Dimer Variation

	$\frac{\partial q_{O=C}}{\partial r_{C=O}}$[a]	$\frac{\partial q_{O\cdots H}}{\partial r_{C=O}}$[a]	dimer $\nu_{C=O}$ freq[b]	dimer $\nu_{C=O}$ IR int[c]	dimer B_u–A_g splitting[b]	monomer–dimer variation $\Delta\nu_{C=O}$[b]	monomer–dimer variation $\Delta r_{C=O}$[d]
			Calculated				
set 1[e]	0.850	0.240	1740	716	70	−36	+0.019
set 2[f]	0.850	0.0	1818	793	36	+42	+0.005
set 3[f]	0.0	0.240	1818	186	7	+42	±0.0
set 4[f]	0.0	0.0	1888	156	6	+112	−0.010
			Observed				
			1754[g]	766[h]	84[g,i]	−23[g,i]	+0.015[j]

[a] In e Å^{-1}. [b] In cm^{-1}. [c] In km mol^{-1}. [d] In Å. [e] The final force field. [f] The dimer geometry was optimized for each of the force fields sets 2–4. [g] Millikan and Pitzer, ref 37. [h] Marêchal, ref 26. [i] Bertie and Michaelian, ref 21. [j] Harmony et al., ref 9.

Table IX. Effects of C=O Stretching Charge Fluxes on Diagonal Force Constants for Dimer and Intermolecular Interactions between Monomer Units

			This Work				
	$\frac{\partial q_{O=C}}{\partial r_{C=O}}$[a]	$\frac{\partial q_{O\cdots H}}{\partial r_{C=O}}$[a]	diagonal force constants $f_{C=O}$[b]	diagonal force constants f_{C-O}[b]	intermolecular interactions $f_{C=O,C=O}$[b]	intermolecular interactions $f_{C-O,C-O}$[b]	intermolecular interactions $f_{C-C,C=O}$[b]
set 1	0.850	0.240	10.45	7.63	−0.281	−0.063	0.120
set 2[c]	0.850	0.0	10.93	7.63	−0.110	−0.064	0.103
set 3[c]	0.0	0.240	10.76	7.63	0.034	−0.063	0.065
set 4[c]	0.0	0.0	11.02	7.63	−0.023	−0.064	0.047
			Others' Work				
			$f_{C=O}$[b]	f_{C-O}[b]	$f_{C=O,C=O}$[b]	$f_{C-O,C-O}$[b]	$f_{C-O,C=O}$[b]
			SCF Energy Gradient Method[d]				
ref 41	9s4p/4s	basis	13.42		−0.3		
ref 43	4-31G	basis			−0.183	−0.107	0.170
ref 49	7s3p/3s	basis	13.67	8.71	−0.050	−0.161	0.146
			Charge–Charge Interaction Model[e]				
ref 43	4-31G	basis			−0.152	−0.043	0.170
ref 43	6-31G	basis			−0.191	−0.071	0.212
ref 43	6-31G**	basis			−0.192	−0.114	0.237
			Empirical Model (Normal Coordinate Analysis)				
ref 16			11.34	6.89	−0.555	−0.200	0.0
ref 50			11.10[f]	7.05[f]	−0.1	−0.1	0.1
ref 51			9.64[g]	8.36[g]	−0.404[g]	0.056[g]	0.128[g]

[a] In e Å^{-1}. [b] In N cm^{-1}. These force constants are in the internal coordinate basis. [c] The geometry minimized by the final force field set 1 is used for the calculations by sets 2–4. [d] Pulay et al., ref 48. [e] The ab initio charges and their fluxes were used. [f] These values were transformed from the Urey–Bradley force field (ref 50) to the general valence force field. [g] These values were transformed from the internal symmetry coordinate space (ref 51) to the internal coordinate space.

by the cyclic redundancy. The resulting intermolecular force constants relevant to the O—C=O group and the diagonal force constants of the C=O and the C—O bonds are compared with the corresponding constants obtained by the ab initio methods[41,43,49] and the standard normal coordinate analyses[16,50,51] in Table IX. Our signs and order of magnitudes of the intermolecular constants in the final calculation roughly coincide with those of the previous authors. Thus, it is concluded that the Coulomb interaction model including the dynamical charge fluxes would predict the proper signs and magnitudes of these interaction force constants. The cooperative effect of the two charge fluxes is clearly noticed in the differences of the interaction constant $f_{C=O,C=O}$ among sets 1 through 4. Finally, the effect of the two charge fluxes on the Coulomb energy will be briefly mentioned. The Coulomb energies calculated by set 1 and set 4 are −92.2 kJ mol^{-1} and −79.0 kJ mol^{-1}, respectively, while set 2 and set 3 give almost the same values of −85.5 ± 1.1 kJ mol^{-1}. This means that the two charge fluxes contribute additively to the stabilization energy of the dimer. Calculation of Raman intensities and extension to higher alkanoic acids will be reported elsewhere.

Acknowledgment. This work was supported by a grand-in-aid for Scientific Research form the Ministry of Education, Science, and Culture (No. 62570964). The calculation in this work was performed on FACOM M-780 computer system in the Data Processing Center, Kyoto University.

Registry No. Formic acid, 64-18-6; formic acid dimer, 14523-98-9.

(48) Pulay, P.; Fogarasi, G.; Pang, F.; Boggs, J. E. *J. Am. Chem. Soc.* **1979**, *101*, 2550.
(49) Karpfen, A. *Chem. Phys.* **1984**, *88*, 415.
(50) Kishida, S.; Nakamoto, K. *J. Chem. Phys.* **1964**, *41*, 1558.
(51) Alfheim, I.; Hagen, G.; Cyvin, S. J. *J. Mol. Struct.* **1971**, *8*, 159.